

Published in final edited form as:

J Comp Neurol. 2012 October 1; 520(14): 3088–3104. doi:10.1002/cne.23134.

The Central Complex of the Flesh Fly, *Neobellieria bullata*: Recordings and Morphologies of Protocerebral Inputs and Small-Field Neurons

James Phillips-Portillo*

Department of Neuroscience, University of Arizona, Tucson, Arizona 85721

Abstract

The central complex in the brains of insects is a series of midline neuropils involved in motor control, sensory integration, and associative learning. To understand better the role of this center and its supply of sensory information, intracellular recordings and dye fills were made of central complex neurons in the fly, *Neobellieria bullata*. Recordings were obtained from 24 neurons associated with the ellipsoid body, fan-shaped body, and protocerebral bridge, all of which receive both visual and mechanosensory information from protocerebral centers. One neuron with dendrites in an area of the lateral protocerebrum associated with motion-sensitive outputs from the optic lobes invades the entire protocerebral bridge and was driven by visual motion. Inputs to the fan-shaped body and ellipsoid body responded both to visual stimuli and to air puffs directed at the head and abdomen. Intrinsic neurons in both of these structures respond to changes in illumination. A putative output neuron connecting the protocerebral bridge, the fan-shaped body, and one of the lateral accessory lobes showed opponent responses to moving visual stimuli. These recordings identify neurons with response properties previously known only from extracellular recordings in other species. Dye injections into neurons connecting the central complex with areas of the protocerebrum suggest that some classes of inputs into the central complex are electrically coupled.

Keywords

electrophysiology; insect brain; central complex; neuroanatomy; simple response properties; *Neobellieria bullata*

Animals depend on information provided by their sensory systems to generate behaviors. However, little is known about the computational substrates that convert sensory information into the behaviorally relevant codes that initiate and control motor outputs. Accumulating evidence suggests that in insects important aspects of this transformation are performed by a discrete, yet interconnected, set of synaptic neuropils: the protocerebral bridge, the fan-shaped body, the ellipsoid body, and the paired noduli (Power, 1943; Williams, 1975; Strausfeld, 1976; Hanesch et al., 1989). Together these are referred to as the *central complex*. Bodian and ethyl gallate histology shows that projections into, within, and

among the structures of the central complex divide these structures into modules and layers (Williams, 1975; Strausfeld, 1976; Hanesch et al., 1989). The central complex is also associated with several satellite neuropils, the most important of which, with respect to information leaving the brain for segmental ganglia, are the paired lateral accessory lobes. In these, outputs from the central complex interact with other major pathways, including heterolateral flip–flop neurons underlying searching actions by silk worm moths (Iwano et al., 2010) and neurons that descend from the brain to motor centers in the thorax and abdomen (Homberg, 1994).

Mass fills of neurons from the thoracic ganglia, and from sensory neuropils in the brain, show no direct connections to the central complex from sensory neuropils, even though early claims were made to the contrary (Goll, 1967; Honegger and Schürmann, 1975). Projections into the central complex arise from neuropils of the superior, inferior, and lateral protocerebrum, all regions of the brain that receive indirect relays from sensory processing areas. In view of such indirect inputs to it, the central complex is likely to receive processed and behaviorally relevant information.

If each insect species is matched (meaning, adapted) to a specific ecology, then, as suggested by Wehner (1987), it may be expected that its sensory and central nervous systems are correspondingly organized to detect and respond to specific sensory elements of that ecology. Might such correspondences be manifest in the organization of central complexes, which in different species show remarkable evolutionary departures from a plesiomorphic ground pattern (Strausfeld, 1999, 2012)? In cockroaches, for example, which are mainly crepuscular or nocturnal and rely greatly on tactile information, Ritzmann et al. (2008) have used extracellular recording techniques to demonstrate that units in the central complex of the cockroach *Blaberus discoidalis* are sensitive to antennal movements, changes in illumination, and in many cases both. In grasshoppers and certain species of butterfly, polarized light is suggested to play an important role in behavior, although what that behavior might be has not yet been established. In the locust *Schistocerca gregaria*, neurons originating from the dorsal rim of the eye and projecting through the optic lobes to a specialized optic glomerulus supply information about the angle of polarized light to various neuropils of the central complex (Vitzhum et al., 2002; Homberg et al., 2003; Homberg, 2004). Sakura et al. (2008) working with the cricket *Gryllus bimaculatus*, and Heinze and Homberg (2009) using the grasshopper *S. gregaria*, also identified neurons in the ellipsoid body that precisely encode polarized light information. Many of the outputs of the central complex extend to paired satellite neuropil, called the **lateral accessory lobes**, associated with processes of premotor descending neurons that reach thoracic ganglia (Wada and Kanzaki, 2005). In the monarch butterfly, comparable systems in modules of the central complex encode information about the distribution of e-vectors across the day-lit sky (Heinze and Reppert, 2011).

In view of the lack of physiological data on polarization sensitivity in the cockroach central complex, or the representation of haptic stimuli in the central complex of locusts or butterflies, it is not yet possible to conclude that the central complex serves the same or different functions in different species. However, that the central complex serves the same functions may be unlikely given that, although different species possess the same classes of

neurons and the same ground pattern of central complex development, their central bodies are variously elaborated, and the number of neurons participating in them differ (Boyan and Reichert, 2010). The central complexes of cockroaches, locusts, butterflies are just three that exemplify a divergent evolution that has occurred in many other insect lineages.

These considerations pose the question of whether central complexes across Insecta share a common functional ground pattern or whether in different species they serve different and specific behavioral functions. What is so far known about the sensory representation in cockroach and locust (or monarch butterfly) central complexes suggests that they might support different roles, but this is still very uncertain.

Thus far, genetic studies on the dipteran *Drosophila melanogaster* have demonstrated a role for some neurons terminating in the central complex in the discrimination of visual features. Tangential neurons projecting into the fan-shaped body are required for recall of an aversive visual stimulus: those encoding stimulus inclination are refractory to stimulus height; those encoding visual height are refractory to stimulus inclination (Liu et al., 2006). Gene expression studies have also shown that neurons terminating in the ellipsoid body of *Drosophila melanogaster* are important for the execution of visual working memory (Neuser et al., 2008), visual place learning (Ofstad et al., 2011), and long-term memory consolidation (Wu et al., 2007). Together, these studies suggest that in *Drosophila* certain neurons in the central complex are required for not only visual behaviors but also many other functions. Genetic intervention, pharmaceutical manipulation, and lesion studies also demonstrate many behavioral attributes of the central complex in a variety of taxa. These include coordinated song production (Orthoptera: Heck et al., 2009; Kunst et al., 2011), locomotory program modulation (*Drosophila*: Kahsai et al., 2010), walking control and maintenance (*Drosophila*: Martin et al., 1999, 2002; Poeck et al., 2008), flight initiation (*Drosophila*: Ilius et al., 2004), alcohol-dependent locomotion and tolerance (*Drosophila*: Kong et al., 2010), obstacle negotiation (Dictyoptera: Harley and Ritzmann, 2010; Bender et al., 2010), maze gravitaxis (*Drosophila*: Baker et al., 2007), courtship (*Drosophila*: Sakai and Kitamoto, 2006), and a range of other voluntary motor actions (Dictyoptera: Gal et al., 2005).

Determining what computational events are common to central complexes will require a broad sampling of central complex physiology and behavioral associations across taxa. Even though responses to, say, linear polarized light by corresponding central complex neuropils in three species is well established, this modality may be less well represented or even unrepresented in others. Indeed, there are no data yet to show that the central complex encodes polarized light information for it to participate in driving a specific behavior. To investigate further what kinds of information are represented in central complexes, this account describes neurons in *Neobellieria bullata*, a dipterous insect distantly related to *Drosophila*, that project to and within central complex neuropils. Although the number of neurons sampled is modest, these are shown to encode information about visual motion, wind perception, and ambient illumination. Several neurons are homologues of those described from the locust and monarch butterfly, but none thus far recorded in *N. bullata* responds to linear polarized light.

MATERIALS AND METHODS

Animals

Pupae of the blowfly *N. bullata* were acquired commercially from Carolina Biological Supply (Burlington, NC). Adult flies were maintained in mesh cages in environmental chambers and provided with powdered milk, sugar, and water ad libitum. Recordings and immunohistochemistry were conducted using primarily male flies between 1 and 3 weeks after eclosion. Occasionally, a female was used for recording when no males were available.

Intracellular recordings

For experiments, adult flies were cold anesthetized and mounted either by the thorax with the legs free so that the animal could walk on a Styrofoam sphere floating in water or restrained in a plastic tube. In both cases, to achieve stability for recordings, the head was fixed by waxing the mouthparts to a support. This allowed control of the head angle and stabilized electrode placement. Access to the brain was achieved by removing a small window of cuticle and the underlying trachea from the back of the head. The perineural sheath was weakened by the application of protease (type XIV from *Streptomyces griseus*, 2 mg/ml in fly saline; Sigma, St. Louis, MO). After removal of the cuticle, the brain was kept moist under fly saline made according to Fayyazuddin and Dickinson (1996). A silver reference electrode was placed through the cuticle in the front of the head under the right eye.

Recording electrodes were pulled from thick-walled borosilicate glass (inside diameter 0.58 mm; World Precision Instruments, Sarasota, FL) on a Sutter P-2000 laser puller (Sutter instruments, Novato, CA). Electrode tips were filled with 4% neurobiotin tracer in 2 M potassium acetate (Vector, Burlingame, CA) and then backfilled with 2 M potassium acetate. With this solution, tip resistance ranged from 60 to 100 M Ω . During recordings, a small negative current was sometimes used to initially stabilize a neuron's firing. After recording, neurobiotin was driven into the neuron with a positive (depolarizing) current of at least 1 nA at 1 Hz for at least 1 minute. Alexa dye was expelled from the recording electrode by using negative (hyperpolarizing) current. After experiments, the tracer was allowed to diffuse throughout the nerve cell for at least 20 minutes while the brain was kept covered with saline solution.

Visual stimuli

Frontal visual stimuli were generated in Vision Egg (Straw, 2008), and displayed via a CRT monitor set at a resolution of 640 \times 480 with a vertical refresh rate of 120 Hz. The monitor was placed 13 cm in front of the animal and subtended 80° horizontally and 60° vertically to the frontal visual field. The monitor was centered in the fly's horizontal visual field and vertically covered 45° above and 15° below the midline of the eyes (Fig. 1A). All of the neurons describe here were tested with a motion stimulus in which a single bar (60° tall and 6° wide) was moving at 64° per second across the monitor, perpendicular to its length, at 45° intervals (Fig. 1B). This stimulus was always presented at maximum contrast, and both a white bar on a black background and a black bar on a white background were tested. These neurons were also tested for responses to the e-vector of polarized light. Polarized light

stimuli were presented from overhead using green, violet, and UV light emitting diodes (LEDs, peak emissions at 476, 404, and 368 nm, respectively; J&E Electronic) projected through a rotatable polarizing filter (B+W Top-Pol; Schneider Optics, Van Nuys, CA). Both stepped changes in orientation and continuous rotation were tested. Each experiment began with stepped changes, using a square wave generator to provide polarized light every second and moving 45° starting at 0° (aligned with the animals body axis). Next, the polarizer was rotated continuously at 36° rotation/second. Each rotation was performed at least twice. Measurements of the spectral content of the POL stimulus measured from the position of the fly's head in the rig showed that the polarization filter did not distort the spectrum in the UV range (USB2000 spectrophotometer; Ocean Optics, Dunedin, FL). The UV peak is small compared with others, but this is due to the UV LEDs commercially available. Other experiments used a broad-spectrum and high-intensity halogen lamp to test for e-vector responses. No responses to the e-vector of polarized light were found using either UV or broad-spectrum and high-intensity stimuli.

The array of LEDs used for polarized light stimulation occupied 1° of the superior visual field. Light flashes from a commercially available incandescent flashlight (advertised 65 lumens; Surefire, Fountain Valley, CA) were used to generate “on” and “off” visual stimuli. Mechanical stimuli in the form of air puffs were delivered through a pipette from left, right, and center for both the head and the abdomen. Although not measured, air puffs were generated in the same manner from experiment to experiment. The velocities of the air currents are assumed to be similar but were not measured. Vibrations from tuning forks at 128, 512, and 1,024 Hz were also tested, but no responses to these were found. The outputs of a photodetector connected to the digitizer were used to align the visual stimuli with the intracellular recordings. The same could not be done for the mechanical stimuli, so precise timing information for these responses is not available.

Histology

Neurobiotin labeling was enhanced with a fluorophore-conjugated streptavidin so that filled neurons could be visualized using confocal microscopy. To better visualize the neuropils contacted by impaled neurons, brains from experimental animals were also labeled using antiserum raised against synaptic proteins. Brains were dissected out in cold 4% formaldehyde in phosphate-buffered saline (PBS; Sigma-Aldrich; pH 7.4), microwaved under vacuum at 18°C, and then allowed to fix overnight at 4°C. Fixed brains were washed several times in PBS and then dehydrated through ascending concentrations of alcohol, permeabilized with propylene oxide, and then rehydrated back into PBS. Tissue was embedded in agarose (type 1A; Sigma-Aldrich) and sectioned at 60 µm. Sections were washed in PBS with 0.5% Triton X-100 (EMS, Hatfield, PA; PBST) and then blocked in 5% normal goat serum (NGS) and PBST. To identify the projection patterns of filled neurons reliably, sections were incubated overnight with an antisynapsin antibody to resolve neuropils (anti-SYNORF1 as described by Klagges, et al., 1996; obtained from the Developmental Studies Hybridoma Bank, University of Iowa, Iowa City, IA) and treated to enhance the neurobiotin signal. For this, sections were again washed and blocked before secondary incubation with a fluorescent antibody (Cy2 anti-mouse, and Cy3 conjugated

streptavidin; both from Jackson ImmunoResearch, West Grove, PA). Afterward, sections were thoroughly washed and mounted with elvanol (Rodriguez and Deinhardt, 1960).

Some early recordings were conducted using Alexa dyes (Alexa 548 or 647 from Invitrogen, Carlsbad, CA) instead of neurobiotin. The general procedure was the same except that these electrodes were filled with concentrated Alexa dye and backfilled with saline. This tissue was fixed overnight in 4% formaldehyde and then embedded in Spurr's high-viscosity embedding media (EMS) and sectioned at 25 μm .

To resolve components of the structural ground pattern of the *N. bullata* central complex, animals were killed and brain tissue processed as above. Sections were labeled with antibodies raised against γ -aminobutyric acid (GABA), FMRFamide, and serotonin (5-HT). When appropriate, these antisera were combined with the antiserum raised against synapsin described above. The substances against which these antisera were raised, manufacturer information, and the concentrations used are listed in Table 1. It should be noted that the antibody used here, raised against FMRFamide, is known to recognize other FaRP peptides, such as myosuppressin, NPF, and sulfakinin (see Nässel, 2002). The staining procedure for this tissue was the same as for injected brains treated with streptavidin and the antiserum raised against synapsin. After washing, bound antibodies were detected using fluorescent secondary antibodies. These antisera are used not to establish a novel localization pattern or for functional identifications but to visualize the organization of the central complex in *N. bullata*.

Antibody characterization

The antisynapsin antiserum was acquired from the Developmental Studies Hybridoma Bank. This antiserum was raised against the conserved 5' sequence of *Drosophila* synapsins as described by Klagges et al. (1996) and cross-reacts with synapsins from many invertebrate species (anti-SYNORF1 data sheet; Developmental Studies Hybridoma Bank). Staining with this antiserum reveals the structures of the central complex and shows its anatomy to be similar to that seen in other dipteran species. For example, examination of the staining pattern that this antiserum produces in the ellipsoid body reveals two distinct regions (an anterior and a posterior ring) that are also seen in *Drosophila* tissue stained with nc82, an antiserum that recognizes the synaptic protein Bruchpilot (Young and Armstrong, 2010).

The anti-FMRFamide antiserum was originally provided by Dr. E. Marder, Brandeis University (Waltham, MA), for use by Dr. I. Sinakevitch (Sinakevitch et al., 2001). In *N. bullata*, this antiserum produces a staining pattern similar to that reported for *Manduca sexta* (Homberg et al., 1990), with bright staining throughout the fan-shaped body and two FMRFamide-like immunoreactive fascicles per side connecting the protocerebral bridge with the fan-shaped body.

The antiserum raised against GABA was affinity purified and characterized by Sigma. This antiserum shows positive binding to both GABA and GABA conjugated to keyhole limpet hemocyanin, but not to bovine serum albumin, in dot-blot immunoassays (Sigma GABA antiserum product information sheet). In the central complex of *N. bullata*, this antiserum labels neurons with a morphology corresponding to that of GABAergic neurons identified in

other publications. Ring neurons of the ellipsoid body with dendrites in the lateral triangle are brightly stained. Similar neurons are labeled by anti-GABA staining in *Drosophila* (Hanesch et al, 1989) and in *M. sexta* (Homberg et al, 1987).

The antiserum raised against serotonin did not react with 5-hydroxytryptophan, 5-hydroxyindole-3-acetic acid, or dopamine in preadsorption controls carried out by the manufacturer (Immunostar 5-HT rabbit antibody data sheet) and in *Neobellieria bullata* produces the same staining pattern in the fan-shaped body as has been reported in *Drosophila* with other antisera raised against serotonin (Kahsai and Winther, 2011).

Reconstruction of neurons

Sections were scanned using a Zeiss LSM 5 confocal microscope (Carl Zeiss, Jena, Germany). Filled nerve cells were reconstructed from these confocal stacks in Adobe Photoshop (Adobe Systems, San Jose, CA), with contrast and brightness manipulated for optimal resolution. For the neurons illustrated in the subsequent figures, image stacks were projected through an LCD projector (Mitsubishi XL1U; Mitsubishi Electric, Tokyo, Japan), reflected by a surface-glazed mirror onto paper, and traced by hand so that the fine details would be reproduced with the same contrast as the brightest profiles.

Data analysis

Analyses of the recorded data were carried out in Matlab (The Mathworks, Natick, MA). Action potential times were extracted from membrane potential recordings by a peak-finding algorithm and verified manually. Stimulus times were extracted from the digitized photodetector channel. For light flash stimuli, spike times were aligned based on the onset of the stimulus and the peristimulus time histogram (PSTH) calculated by binning spikes into 5-msec bins and convolving that histogram with a 25-msec Gaussian window, as described by Paulk et al. (2008). Directional and orientation preferences for were calculated using the Rayleigh test as described by Batschelet (1981).

Nomenclature

Throughout this account, neurons and brain structures are viewed in frontal sections. *Anterior/posterior* and *superior/inferior* describe relative positions with respect to the body axis. *Rostral/caudal* and *dorsal/ventral* refer to the neuraxis. A frontal section is one cut perpendicular to the body axis but parallel with the neuraxis.

Module refers to divisions across the fan-shaped or ellipsoid body imposed by small neurons linking them with the protocerebral bridge. The fan-shaped body is composed of an upper and a lower division, each composed of succession of strata. Divisions of the superior protocerebrum and other regions are named according to nomenclature determined for the *Drosophila* brain (Ito et al., 2012). The term *RF tract* (Hanesch et al., 1989) is here abbreviated to *RT*, for “ring neuron tract.”

RESULTS

Anatomy and chemical organization of the central complex in *Neobellieria bullata*

Intracellular recordings using dye-filled electrodes were attempted from 200 flies. Twenty-four neurons were filled that showed major arbors in at least one structure of the central complex. The morphology and spiking responses of nerve cells to visual and mechanosensory stimuli are described below, and a summary of the recorded neurons and their responses is shown in Table 2.

The application of just four antisera provided useful neuroanatomical data for identifying the ground pattern organization of these neuropils and salient features of the internal architecture, all of which correspond to descriptions of the central complex of *D. melanogaster* (Hanesch et al., 1989; Kahsai and Winther, 2011). Labeling of the brain with antibodies raised against synapsins demonstrates the modular cytoarchitectonics of central complex neuropils, clearly distinguishing it from the surrounding tissue. The central complex comprises four distinct neuropils: the protocerebral bridge, the fan-shaped body, the ellipsoid body, and the paired noduli (Fig. 2A,B). The neuropils of the central complex appear as distinct synaptic regions, with the fan-shaped body clearly divided into upper and lower components, the latter more densely equipped with synapses. Both reveal their modular organization into repeated subunits across their extent. The protocerebral bridge has the highest density of antisynapsin labeling. The noduli, which lie immediately beneath the fan-shaped body, are subdivided into three distinct synaptic regions (Fig. 2F). The ellipsoid body, disposed in front of the fan-shaped body (ventral to it according to the neuraxis) is divided into a somewhat dense inner ring and a more diffuse outer ring (Renn et al., 1999), which, in Young and Armstrong's (2010) terminology for *Drosophila*, are the anterior (A) and posterior (P) rings.

Labeling with other antisera further reveals central complex architecture. In *N. bullata*, as in *Drosophila* (Hanesch et al., 1989), GABA-like immunoreactivity is more prominent in the ellipsoid body than in any other central complex neuropil. The morphology of GABA-like immunoreactive projections into the ellipsoid body corresponds to that of the ring neurons: antibodies raised against GABA strongly label the neurites in the RT (Hanesch et al., 1989) and the whole of the ellipsoid body. Figure 2D shows a transverse section through the fan-shaped body, ellipsoid body, and the RT at a level that shows the stratum of GABA-like immunoreactivity in the fan-shaped body. Notably, these neurons completely occlude the modular organization of the fan-shaped body. The dendritic branches of the labeled ring neurons also reveal the small satellite neuropils now known as the *bulbs* (BU; see Ito et al., 2012).

The ellipsoid body, noduli, and fan-shaped body all contain networks of large fibers that show 5HT-like immuno-reactivity (Fig. 2E,F). Conspicuously, the protocerebral bridge is devoid of 5HT-like immunoreactivity (Fig. 2G). A similar lack of 5HT-like immunoreactive fibers has been reported in studies on *Drosophila* (Kahsai and Winther, 2011).

In contrast to anti-GABA staining, labeling of the central complex with antisera raised against the neuropeptide FMRFamide reveals the distinctive repeat organization of eight

modules across the fan-shaped body. Bundles of FMRFamide-like immunoreactive fibers can also be seen connecting modules with each other (Fig. 2H). The protocerebral bridge and ellipsoid body are, however, devoid of FMRFamide-like immunoreactivity (not shown here).

Neuron morphologies and responses

Widefield projections supplying the protocerebral bridge—The protocerebral bridge receives an input from a prominent neuron, equipped with a 4–6 μm diameter axon, the dendrites of which reside in the ventrolateral protocerebrum and originate from a cell body near the esophageal foramen (Fig. 3A). Its dendrites extend to the deepest levels of optic lobe outputs (Strausfeld and Lee, 1991). These are optic glomeruli receiving terminals of retinotopic neurons from the lobula complex (see Strausfeld and Okamura, 2007) and the axonal collaterals of motion-sensitive neurons that extend centrally from the lobula plate (see Strausfeld and Bassemir, 1985). Regions of the brain receiving axons from the optic lobes can be distinguished by virtue of those axons being immunonegative to antisynapsin and standing out as dark profiles in confocal sections. Dendrites extend among optic glomeruli. In the close relative dipteran *Phaenicia sericata*, these are known to receive outputs from edge-motion-sensitive neurons from the lobula plate and lobula (Okamura and Strausfeld, 2007). Other dendrites extend lateroventrally to reach the prominent axon collaterals of horizontal-motion-sensitive neurons from the lobula plate (Fig 3A, inset). A thick axon projects medially toward the esophagus and then abruptly ascends posterodorsally to reach the protocerebral bridge. The axon bifurcates beneath the protocerebral bridge to provide a system of branches throughout its entire extent. The branches provide many fine collaterals decorated with bead-like swellings. This cell type was encountered a second time in another preparation, in which several neurons were filled during multiple recordings.

The neuron showed a resting membrane potential of approximately -45 mV, a spike amplitude of nearly 50 mV, and a background firing rate of six impulses per second. The neuron responded with a brief (approximately 100 msec) increase in firing rate to both the initiation and the termination of a light flash both for plane polarized and for unpolarized light (Fig. 3B). However, the neuron showed no selective response to polarized light: the magnitudes of “on” and “off” responses were independent of the e-vector. With a rotating polarizer, no firing rate modulation could be detected beyond the initial on response and terminal off, which were of equal magnitude.

For a bright bar 60° tall and 6° wide moving at $64^\circ/\text{second}$, the neuron responded with an increase in firing rate that persisted for approximately 500 msec. No off response was apparent when the bar moved along this cell's preferred direction, as shown in Figure 3C. When the bar moved along the antipreferred direction the cell's firing rate was indistinguishable from its spontaneous firing rate. The directional preference of this cell for moving bars is plotted in Figure 3D; the gray circle represents the background firing rate ± 2 standard deviations, and the black trace represents the magnitude of the response averaged over the entire period for which the bar moved in each direction. Although the firing rate of this cell in response to a bar moving along its preferred direction is different from its

unstimulated rate (Fig. 3C,D), the shape of the resulting directional preference distribution is not significantly different from random by the Rayleigh test ($n = 193$, $r = 0.084$, $P > 0.1$; Fig. 3D). This cell appeared to have a large receptive field, because no position of the moving bar elicited greater activity than any other, and the neuron responded with the same magnitude to light flashes given to any part of the eye.

Tangential neurons linking the superior protocerebrum and fan-shaped body

—Neurons with arbors that span the width of the fan-shaped body were the most common cell type encountered. Fourteen neurons were recorded and filled (in as many preparations), all of which had their perikarya in the lateral cell body layer between the calyx and the optic lobes. Their arborizations occupied different and discrete domains of the superior protocerebrum (see Phillips-Portillo and Strausfeld, 2012). Their axons project from the protocerebrum to the edge of the fan-shaped body or over its outermost layer, where they give rise to many terminal collaterals decorated with presynaptic boutons and varicosities (Fig. 4A,B).

Several of these neurons ($n = 4$) were filled with Alexa dyes, which allowed a clear reconstruction of each of their individual morphologies (Fig. 4A). In experiments in which neurobiotin was used as a tracer, several neurons ($n = 10$) having the same morphology and derived from a common cell body cluster were filled together (Fig. 4B, inset). Because this happened consistently when using neurobiotin and because neurons of equivalent morphology were filled, such a collective demonstration is unlikely to be to the consequence of accidental penetration of many neurons in the same preparation. Rather, fills into identical nerve cells in the same brain is indicative of dye coupling (see Discussion). In these cases, the intensity of staining and the clarity of the cell bodies indicate that at least eight neurons of this type originate on each side of the brain. Because both contralateral and ipsilateral pairs of neurons are filled by dye injection into a single cell, dye coupling must occur in the fan-shaped body, because this is the only place where neurons from both sides of the brain overlap.

These tangential neurons exhibited background firing rates between 5 and 15 impulses/second and typical action potential of over 40 mV. Recordings from these neurons were in general very stable, which allowed the presentation of a wide variety of stimuli. However, only one neuron demonstrated a clear response to any of the presented visual or mechanosensory stimuli. This nerve cell responded with an increase in firing rate to light flashes (Fig. 4F) and with a brief burst of action potentials when puffs of air were directed at the front of the head. Figure 4G shows the response of this neuron when air currents were pulsed in various directions across the head. For comparison with the other cell types described here, an example of the direction preference plot for a tangential neuron is presented in Figure 4H. This cell had a mean firing rate of 13 impulses/second, with a standard deviation of 1 impulse/second (Fig. 4E). The firing rate for every direction of the stimulus falls within two standard deviations from the mean, and the shape of the resulting distribution is not significantly different from a uniform distribution as calculated by the Rayleigh test ($n = 257$, $r = 0.006$, $P > 0.05$). For the other neurons with this generic morphology, spike frequency and spike timing analyses failed to reveal any stimulus related spiking patterns, and analysis of the subthreshold membrane activity similarly failed to show

voltage changes reliably associated with any stimulus parameter presented to the animal. However, in one tangential neuron, a transient switch to firing spike doublets (Fig. 4C,D) was correlated with the switch from one submodality to another and, subsequently, when the ambient illumination was turned on or off (Fig. 4I, arrow).

Pontine neurons supplying the fan-shaped body and ellipsoid body—Narrow clusters of axons, dendrites, and terminals project through the stratified organization of the fan-shaped body. Among these are the narrow terminals of neurons that project into the fan-shaped body from the protocerebral bridge. These projections contribute to the division of the fan-shaped body into modules. Different levels of these modules are interconnected by one type of a class of interneurons called *pontine neurons* by Hanesch et al. (1989). Other pontine neurons connect modules laterally. Results of recording from four of these neurons are described below.

The most stable recordings of pontine neurons demonstrated a resting membrane potential of approximately -40 mV and large spikes, up to 50 mV in amplitude with average firing rates between 4 and 12 impulses/second. As with protocerebral bridge neurons, changes in luminance best drive these nerve cells, independent of wavelength or the e-vector of polarization. All of these nerve cells exhibited excitatory responses to increases in illumination. One pontine neuron, illustrated in Figure 5A–D, fired a brief excitatory burst to the onset of light flashes, similar to that seen in the motion-sensitive protocerebral bridge input. Judged from the peristimulus time histogram, this response lasted on the order of 100 msec. There was no following off response, however (Fig. 5C,D). Although this neuron was one of two pontine neurons that connected two strata within a module, such transient responses are atypical. All other recorded pontine neurons responded to increases in luminance with excitatory responses that persisted as long as the stimulus was present, as in the peristimulus time histogram shown in Figure 5E.

The motion sensitivity of these neurons was also tested. Directional tuning for a white bar moving on a black background is illustrated in Figure 5F. The stimulated firing rate surpasses 2 standard deviations above the mean when the bar is moving to the left, and, in comparing the firing rates elicited for all directions, the distribution is significantly different from uniformity (Rayleigh test, $n = 202$, $r = 0.16$, $P < 0.01$).

Pontine neurons exhibited the most variable baseline firing rates of any of the recorded neurons. The neuron shown in Figure 5A–D had a mean firing rate of 5 impulses/second calculated over the length of the recording. However, the raster plot shows extended periods in which the firing rate was as high as 10–12 impulses/second and others in which it was as low as 1 impulse/second. Interestingly, these neurons have periods during which they cease to respond to visual stimuli that at other times elicit a strong response. In Figure 5D, for example, the raster plot shows periods in which light flashes failed to produce a response. Although these neurons are responsive to visual stimuli, their activity appears to be influenced by factors outside those controlled in these experiments.

One recording was also obtained from a pontine neuron associated with the ellipsoid body. Like the neurons described above, this nerve cell had a resting membrane potential of -45

mV, spike amplitudes of over 60 mV, and a mean firing rate of approximately 5 impulses/second. Like the fan-shaped body interneuron shown in Figure 5C, this nerve cell demonstrated a narrow response to the onset of changes in illumination and no off response.

Ring neurons of the ellipsoid body—Two ring neurons, the principal cells of the ellipsoid body (Renn et al., 1999), were recorded from and filled in these experiments. The first of these had its cell body near the esophageal foramen, posterior to the antennal lobes. It was equipped with a small tuft of processes beneath and anterior to the mushroom body medial lobe, in an area of the protocerebrum named the *crepine* (CRE; see Ito et al., 2012), and varicose terminals throughout the posterior ring of the ellipsoid body (Fig. 6A,B). This morphology is similar to that of the ExR2 neurons described by Hanesch et al. (1989), in that this neuron has blebbed arborizations in the posterior ring of the ellipsoid body, a small set of putative inputs in the protocerebrum (instead of the bulbs), and a ventrally projecting cell body fiber.

As with the tangential neurons illustrated in Figure 4, ring neurons are possibly dye coupled with each other, because, when one is filled, a second cell body accompanies that of the filled neuron, and contralaterally there is a pair of cell bodies in the corresponding location, both providing a neurite to the ellipsoid body. In the illustrated example (Fig. 6A,B), the recorded neuron is brightly labeled, accompanied by a more weakly labeled contralateral counterpart entering the ellipsoid from the opposite side. Figure 6B shows the bright neurobiotin-labeled neurite and ellipsoid body branches of the recorded neuron reconstructed in Figure 6A, with an accompanying ipsilateral perikaryon and a pair of contralateral perikarya, one very faintly but unambiguously labeled (upper inset, Fig. 6B). Anatomically, branches in the ellipsoid body are uniformly blebbed, suggesting that this arbor is an axon terminal. Branches in the bulb of the accessory lobe are decorated with spicules, suggestive of a postsynaptic arbor.

The recorded neuron reconstructed had a resting membrane potential between -45 and -50 mV and action potentials with amplitudes of about 35 mV. It fired rapidly, with a mean firing rate of 28 impulses/second (Fig. 6C). In general, the firing rate of the neuron varied on a finer time scale than that seen in pontine neurons. Irrespective of whether light was polarized, repeated presentations of light flashes revealed a subtle excitatory response to increases in illumination (Fig. 6D). The increased spike probability in this neuron lasts for the duration of the stimulus, although in several stimulus presentations the background firing rate was unaffected. Spontaneous lulls in firing can be seen in the voltage trace shown in Figure 6C. This again may indicate that this neuron's firing is influenced by a sensory modality or a process that is independent of the presented stimulus. The neuron showed no sensitivity to the e-vector of polarized light (Rayleigh test, $n = 596$, $r = 0.007$, $P > 0.05$; data not shown) or to moving bars (Fig. 6E; Rayleigh test, $n = 67$, $r = 0.1$, $P > 0.05$) or to the orientation of stationary or moving bars (Rayleigh test, $n = 67$, $r = 1.8$, $P > 0.05$).

The second recorded ring neuron originated from a cell body located anterior to (above) the protocerebral bridge, in the pars intercerebralis. The cell body gives rise to a single neurite that projects anteriorly and downward to reach the front of the fan-shaped body, just above the upper margin of the ellipsoid body. There, the neurite bifurcates to form two stout

branches that each send relatively sparse projections down into the ellipsoid body and to the lateral accessory lobes (Fig. 6F).

This neuron had a resting membrane potential of approximately -30 mV and action potentials of approximately 45 mV in amplitude. As with the other ring neuron described above, it responded to light flashes with a brief increase in firing rate, lasting for approximately 100 msec (Fig. 6G). Although the first light flash presented to this cell (first row in the rastergram) elicited the most robust response, the increase in firing rate for the other trials still exceeded 2 standard deviations above the background rate. The stimulus presentations shown in Figure 6G are taken from different periods throughout the recording. As with the pontine neurons, the response of this cell to changes in illumination varies throughout the recording, independent of the parameters of the presented visual stimuli. This neuron also produced a clear response to nonvisual stimuli. This cell responded strongly to air puffs directed at the animal's head from all the directions with a large increase in firing rate that lasted for several hundred milliseconds. Figure 6H shows the response of this cell to two air puffs presented frontally in rapid succession (arrows).

Connection of the protocerebral bridge, fan-shaped body, and lateral accessory lobes

—One recording and dye fill demonstrated a neuron linking these three neuropils. The neuron originates from a cell body in the pars intercerebralis and has dendritic spines in the protocerebral bridge. Its processes are restricted to one module of the fan-shaped body, where they provide mixed varicose and spiny processes. It terminates in the contralateral lateral accessory lobe, where it provides beaded axon branches (Fig. 6I). The distance between the branches in the protocerebral bridge and the lateral edge of that neuropil places its arbors in the second and third modules of the right side of the protocerebral bridge and thus within the most medial module of the left side of the fan-shaped body. This arborization pattern corresponds to a projection of the “Y” bundle of the horizontal fiber system described by Hanesch et al. (1989) from observations of *Drosophila*. The neuron showed a resting membrane potential of -35 mV and very large spikes of over 80 mV in amplitude (Fig. 6J). Its background firing rate varied between 4 and 9 impulses/second. During recording, the fly was presented with polarized and unpolarized light stimuli from overhead and drifting bars and gratings. However, the recording was not of sufficient duration to allow presentation of nonvisual stimuli.

The neuron did not respond to brief changes in illumination (Fig. 6K), nor did it respond to the e-vector of plain polarized light. However, the observed firing rate during the long periods (approximately 50 sec) when a dark bar was periodically displayed on the white CRT screen doubled (from 4 impulses/second to 9 impulses/second). However, other than this response, the neuron did not react to any of the stimuli presented with unambiguous and significant changes in firing rate. Its response to a black bar moving on a white background is evident only when the responses to several directions are compared with the background firing rate (Fig. 6L). The shape of this distribution is significantly different from uniform (Rayleigh test, $n = 170$, $r = 0.158$, $P < 0.05$). The calculated background firing rate for this period of the recording is high (10 impulses/second with a standard deviation of 3 impulses/second) as calculated by the average number of spikes recorded when no stimulus was presented. The firing rate during stimulus presentations was also variable, as evidenced by

the difference between firing rates for repeated trials. Interestingly, this difference is smallest for the preferred direction and minimal in the antipreferred direction. This directional response pattern is similar to that seen in the protocerebral input neuron shown in Figure 3, suggesting that protocerebral bridge inputs may contribute to this cell's activity. However, other signals clearly must be contributing to this nerve cells activity, because, when the neuron fires without reference to a presented stimuli, its firing rate alternates between periods of sporadic spiking activity and bursts of spikes, implying that the neuron is responding to some ongoing input in addition to the visual stimuli presented.

DISCUSSION

Multiple neurons labeled: damage or dye coupling?

An interesting feature of the class of ring neurons and tangential neurons is that several neurons of the same type can be labeled when recording from a single cell, using neurobiotin as the neuronal tracer. All 10 neurobiotin fills of tangential neurons revealed an ensemble of neurons, whereas such multiple labeling was not seen in volumes of the protocerebrum not associated with the central complex. Also, multiple fills were never seen in recordings using Alexa dyes. If multiple neurons were labeled as the result of damage, the occurrence of multiple fills would not be expected to be correlated with the type of tracer used. Moreover, tangential neurons showed very stable resting membrane potentials and in general large, consistent spike amplitudes during the entire recording session. These aspects suggest minimal damage to the impaled neuron. Some recordings showed bouts of bursting activity, in which two or more spikes were produced, separated by a very short latency. In such instances, voltage increases with amplitudes smaller than individual action potentials were observed (Fig. 4C). Action potentials with different heights are often a sign that more than one neuron has been impaled. The occurrence of this activity, however, was not correlated with the number of neurons labeled and was observed even in preparations in which only one neuron was filled.

How species specific is tuning by the central complex?

Intracellular recordings made from a sample of neurons projecting into and within the central complex of the flesh fly, *Neobellieria bullata*, provide little evidence that in this dipteran nerve cells of the complex readily respond to a simple sensory stimulus. This contrasts with findings from locusts and monarch butterflies. In those taxa, a variety of central complex neurons are tuned specifically to the e-vector distribution of polarized light.

Nevertheless observations reported here complement results obtained from a dictyopteran species, *Blaberus discoidalis*. In their study of its antennal sensitive neurons, Ritzmann et al. (2008) report that the majority of antennal mechanosensitive units found in the fan-shaped and ellipsoid bodies are sensitive to changes in illumination. The intracellular recordings of fly neurons described here include similar polysensory responses by certain inputs to the ellipsoid body and fan-shaped body. One extrinsic ring neuron of the ellipsoid body (Fig. 6F–H) showed a phasic response to flashes of light but was more strongly driven by air puffs to the head, likely sensed through the antennae. A similar response was found in a tangential neuron that connects a domain of the superior medial protocerebrum with the fan-

shaped body. This neuron responded to both changes in illumination and air currents (Fig. 4F,G), but, unlike the polysensory ring neuron, it also responded to air puffs to the abdomen. Ritzmann et al. (2008) also report that most light-sensitive neurons in the central complex display phasic responses to changes in illumination. The only tonic responses to light observed by these authors were recorded from the fan-shaped body. This was also the case in *N. bullata*: light-sensitive neurons associated with the ellipsoid body showed only brief responses to changes in illumination. Only pontine neurons of the fan-shaped body showed an increase in firing rate that persisted for as long as the stimulus was present (Fig. 5).

However, important morphological and physiological differences were also observed. In the locust *Schistocerca*, neurons sensitive to the e-vector of polarized light project into the protocerebral bridge in an organized fashion, giving rise to discrete domains of arborization that map all e-vector orientations across the bridge (Heinze and Homberg, 2007). This information is also relayed, albeit with less fidelity, to neurons connecting the bridge to the central body and the lateral accessory lobes. In the present study, inputs to the protocerebral bridge were not sensitive to the e-vector of polarized light but did respond to other kinds of visual stimuli. For example, one input to the protocerebral bridge arising from the optic glomerular complex in the ventrolateral protocerebrum increased its firing rate in response to moving edge stimuli. The terminal of this neuron is not restricted to small domains of the bridge, as are polarization-sensitive neurons in locusts, but extends across all the bridge's modules, as shown in Figure 3.

More generally, several neurons described in this account showed only subtle responses to a given stimulus, and many had long quiescent periods during which they stopped responding to any stimulus at all. Heinze and Homberg (2009) report a similar phenomenon in some polarization-sensitive neurons in the locust. They conclude that neurons may be recruited into a polarization vision network in a task-specific manner or possibly depending on the internal state of the animal. Those authors pointed out that, because the central complex has a role both in sensory processing and in motor control, changes in response properties should be expected, because motor action will influence sensory parameters. In the present study, fluctuations in response properties over a slower time scale were observed during some longer recordings, such as by pontine neurons of the fan-shaped body (see Fig. 5D). These slower changes may be due to neuromodulatory influences on the central complex and may thus depend more on the internal state of the animal than on the recording conditions.

Not all of the neurons recorded could be reliably driven by the presented stimulus. Tangential neurons (see Phillips-Portillo and Strausfeld, 2012) maintained a relatively constant firing rate, independent of presented visual or mechanosensory stimuli. In only two such recordings could spiking activity be correlated with any experimental manipulation, namely, a response to both visual and mechanosensory stimuli. This lack of reaction to simple stimuli should not be surprising, however. As shown in *D. melanogaster*, tangential neurons in the outer layer of the fan-shaped body discriminate more structured visual cues than any of those used here (see Liu et al., 2006).

In conclusion, it is likely that visual inputs in the protocerebrum to tangential neurons that terminate in the fan-shaped body, either directly or via the superior protocerebrum, carry information that is matched to ecological constraints of that particular species. In the case of the cockroach, dimming and brightening are relevant visual stimuli, as are haptic stimuli. In the case of the migratory locust and monarch butterfly, skylight polarization may be far more relevant to these species than it is to a cockroach or a fly. On the other hand, in flies, inputs to the protocerebral bridge from optic glomeruli and the terminals of lobula plate tangential cells relay information about visual motion, which has great importance for that taxon's behavioral repertoire.

Acknowledgments

The author thanks Nicholas Strausfeld (University of Arizona, Tucson, AZ) for help and advice in assembling this account and Patrick Williams (Muhlenberg College, Allentown, PA) and Gabriella Wolff (University of Arizona, Tucson, AZ) for their suggestions.

Grant sponsor: National Institutes of Health; Grant number: NCRR RO1-RR008688 (to N.J. Strausfeld); Grant sponsor: NIGMS T32 Gm08400; Grant sponsor: Research to Prevent Blindness Foundation; Grant sponsor: Graduate Program in Physiological Sciences University of Arizona, Tucson.

Abbreviations

CA	Calyx
CRE	Crepine
BU	Bulb
EB	Ellipsoid body
ES	Esophagus
FB	Fan-shaped body
FBI	Lower division of the fan-shaped body
FBu	Upper division of the fan-shaped body
HS	Horizontal cell axons
LAL	Lateral accessory lobe
LOP	Lobula plate
LP	Lateral protuberance
OGC	Optic glomerular complex
SE	Subesophageal ganglion
SMP	Superior medial protocerebrum
NO	Noduli
PED	Pedunculus
PB	Protocerebral bridge
PI	Pars intercerebralis

RT	Ring neuron tract
VS	Vertical cell axons

LITERATURE CITED

- Baker DA, Beckingham KM, Armstrong JD. Functional dissection of the neural substrates for gravitaxic maze behavior in *Drosophila melanogaster*. *J Comp Neurol*. 2007; 501:756–764. [PubMed: 17299758]
- Batschelet, E. Circular statistics in biology. Academic Press; London: 1981.
- Bender JA, Pollack AJ, Ritzmann RE. Neural activity in the central complex of the insect brain is linked to locomotor changes. *Curr Biol*. 2010; 20:921–926. [PubMed: 20451382]
- Boyan GS, Reichert H. Mechanisms for complexity in the brain: generating the insect central complex. *Trends Neurosci*. 2010; 34:247–257. [PubMed: 21397959]
- Fayyazuddin A, Dickinson MH. Haltere afferents provide direct, electrotonic input to a steering motor neuron in the blowfly, *Calliphora*. *J Neurosci*. 1996; 16:5225–5232. [PubMed: 8756451]
- Gal R, Rosenberg LA, Libersat F. Parasitoid wasp uses a venom cocktail injected into the brain to manipulate the behavior and metabolism of its cockroach prey. *Arch Insect Biochem Physiol*. 2005; 60:198–208. [PubMed: 16304619]
- Goll W. Strukturuntersuchungen am Gehirn von *Formica*. *Z Morph Okol Tiere*. 1967; 59:143–210.
- Hanesch U, Fischbach K-F, Heisenberg M. Neuronal architecture of the central complex in *Drosophila melanogaster*. *Cell Tissue Res*. 1989; 257:343–366.
- Harley CM, Ritzmann RE. Electrolytic lesions within central complex neuropils of the cockroach brain affect negotiation of barriers. *J Exp Biol*. 2010; 213:2851–2864. [PubMed: 20675555]
- Heck C, Kunst M, Härtel K, Hülsmann S, Heinrich R. In vivo labeling and in vitro characterisation of central complex neurons involved in the control of sound production. *J Neurosci Methods*. 2009; 183:202–212. [PubMed: 19583981]
- Heinze S, Homberg U. Maplike representation of celestial e-vector orientations in the brain of an insect. *Science*. 2007; 315:995–997. [PubMed: 17303756]
- Heinze S, Homberg U. Linking the input to the output: new sets of neurons complement the polarization vision network in the locust central complex. *J Neurosci*. 2009; 29:4923–4933.
- Heinze S, Reppert SM. Sun compass integration of skylight cues in migratory monarch butterflies. *Neuron*. 2011; 69:345–358. [PubMed: 21262471]
- Homberg U. Flight-correlated activity changes in neurons of the lateral accessory lobes in the brain of the locust *Schistocerca gregaria*. *J Comp Physiol A*. 1994; 175:597–610.
- Homberg U. In search of the sky compass in the insect brain. *Naturwissenschaften*. 2004; 91:199–208. [PubMed: 15146265]
- Homberg U, Kingan TG, Hildebrand JG. Immunocyto-chemistry of GABA in the brain and suboesophageal ganglion of *Manduca sexta*. *Cell Tissue Res*. 1987; 248:1–24. [PubMed: 3552234]
- Homberg U, Kingan TG, Hildebrand JG. Distribution of FMRFamide-like immunoreactivity in the brain and suboesophageal ganglion of the sphinx moth *Manduca sexta* and colocalization with SCPB-, BPP-, and GABA-like immunoreactivity. *Cell Tissue Res*. 1990; 259:401–419. [PubMed: 2180574]
- Homberg U, Hofer S, Pfeiffer K, Gebhardt S. Organization and neural connections of the anterior optic tubercle in the brain of the locust *Schistocerca gregaria*. *J Comp Neurol*. 2003; 462:415–430. [PubMed: 12811810]
- Honegger H-W, Schürmann FW. Cobalt sulphide staining of optic fibres in the brain of the cricket, *Gryllus campestris*. *Cell Tissue Res*. 1975; 159:213–225. [PubMed: 50137]
- Ilius M, Wolf R, Heisenberg M. The central complex of *Drosophila melanogaster* is involved in flight control: studies on mutants and mosaics of the gene ellipsoid-body-open. *J Neurogenet*. 1994; 9:189–206. [PubMed: 7965387]

- Ito K, Shinomiya K, Armstrong D, Boyan G, Hartenstein V, Harzsch S, Heisenberg M, Homberg U, Jenett A, Keshishian H, Restifo L, Rössler W, Simpson J, Strausfeld NJ, Strauss R, Vosshall LB. A coordinated nomenclature system for the insect brain. *Neuron*. 2012 (in press).
- Iwano M, Hill ES, Mori A, Mishima T, Mishima T, Ito K, Kanzaki R. Neurons associated with the flip-flop activity in the lateral accessory lobe and ventral protocerebrum of the silkworm moth brain. *J Comp Neurol*. 2010; 518:366–388. [PubMed: 19950256]
- Kahsai L, Winther AME. Chemical neuroanatomy of the *Drosophila* central complex: distribution of multiple neuropeptides in relation to neurotransmitters. *J Comp Neurol*. 2011; 516:290–315. [PubMed: 21165976]
- Kahsai L, Martin JR, Winther AM. Neuropeptides in the *Drosophila* central complex in modulation of locomotor behavior. *J Exp Biol*. 2010; 213:2256–2265. [PubMed: 20543124]
- Klagges BRE, Heimbeck G, Godenschwege TA, Hofbauer A, Pflugfelder GO, Reifegerste R, Reisch D, Schaupp M, Buchner S, Buchner E. Invertebrate synapsins: a single gene codes for several isoforms in *Drosophila*. *J Neurosci*. 1996; 16:3154–3165. [PubMed: 8627354]
- Kong EC, Woo K, Li H, Lebestky T, Mayer N, Sniffen MR, Heberlein U, Bainton RJ, Hirsh J, Wolf FW. A pair of dopamine neurons target the D1-like dopamine receptor DopR in the central complex to promote ethanol-stimulated locomotion in *Drosophila*. *PLoS One*. 2010; 5:e9954. [PubMed: 20376353]
- Kunst M, Pförtner R, Aschenbrenner K, Heinrich R. Neurochemical architecture of the central complex related to its function in the control of grasshopper acoustic communication. *PLoS One*. 2011; 6:e25613. [PubMed: 21980504]
- Liu G, Seiler H, Wen A, Zars T, Ito K, Wolf R, Heisenberg M, Liu L. Distinct memory traces for two visual features in the *Drosophila* brain. *Nature*. 2006; 436:551–556. [PubMed: 16452971]
- Martin JR, Raabe T, Heisenberg M. Central complex substructures are required for the maintenance of locomotor activity in *Drosophila melanogaster*. *J Comp Physiol A*. 1999; 185:277–288. [PubMed: 10573866]
- Martin JR, Faure F, Ernst R. The power law distribution for walking-time intervals correlates with the ellipsoid-body in *Drosophila*. *J Neurogenet*. 2002; 15:1–15.
- Nässel DR. Neuropeptides in the nervous system of *Drosophila* and other insects: multiple roles as neuromodulators and neurohormones. *Prog Neurobiol*. 2002; 68:1–84. [PubMed: 12427481]
- Neuser K, Triphan T, Mronz M, Poeck B, Strauss R. Analysis of a spatial orientation memory in *Drosophila*. *Nature*. 2008; 453:1244–1248. [PubMed: 18509336]
- Ofstad TA, Zuker CS, Reiser MB. Visual place learning in *Drosophila melanogaster*. *Nature*. 2011; 474:204–207. [PubMed: 21654803]
- Okamura J-Y, Strausfeld NJ. Visual system of calliphorid flies: motion- and orientation-sensitive visual interneurons supplying dorsal optic glomeruli. *J Comp Neurol*. 2007; 500:189–208. [PubMed: 17099892]
- Paulk AC, Phillips-Portillo J, Dacks AM, Fellous JM, Gronenberg W. The processing of color, motion, and stimulus timing are anatomically segregated in the bumblebee brain. *J Neurosci*. 2008; 28:6319–6332. [PubMed: 18562602]
- Phillips-Portillo J, Strausfeld NJ. Representation of the central body of the flesh fly *Neobellieria bullata* in the brain's superior protocerebrum. *J Comp Neurol*. 2012 (in press).
- Poeck B, Triphan T, Neuser K, Strauss R. Locomotor control by the central complex in *Drosophila*—an analysis of the tay bridge mutant. *Dev Neurobiol*. 2008; 68:1046–1058. [PubMed: 18446784]
- Power ME. The brain of *Drosophila melanogaster*. *J Morphol*. 1943; 72:517–559.
- Renn SC, Armstrong JD, Yang M, Wang Z, An X, Kaiser K, Taghert PH. Genetic analysis of the *Drosophila* ellipsoid body neuropil: organization and development of the central complex. *J Neurobiol*. 1999; 41:189–207. [PubMed: 10512977]
- Ritzmann RE, Ridgel AL, Pollack AJ. Multi-unit recording of antennal mechano-sensitive units in the central complex of the cockroach, *Blaberus discoidalis*. *J Comp Physiol A*. 2008; 194:341–360.
- Rodriguez J, Deinhardt F. Preparation of a semipermanent mounting medium for fluorescent antibodies studies. *Virology*. 1960; 12:316–317. [PubMed: 13742591]

- Sakai T, Kitamoto T. Differential roles of two major brain structures, mushroom bodies and central complex, for *Drosophila* male courtship behavior. *J Neurobiol.* 2006; 66:821–834. [PubMed: 16673386]
- Sakura M, Lambrinos D, Labhart T. Polarized skylight navigation in insects: model and electrophysiology of e-vector coding by neurons in the central complex. *J Neurophysiol.* 2008; 99:667–682. [PubMed: 18057112]
- Sinakevitch I, Farris SM, Strausfeld NJ. Taurine-, aspar-tate- and glutamate-like immunoreactivity identifies chemically distinct subdivisions of Kenyon cells in the cockroach mushroom body. *J Comp Neurol.* 2001; 439:352–367. [PubMed: 11596059]
- Strausfeld, NJ. Atlas of an insect brain. Springer-Verlag; Heidelberg: 1976.
- Strausfeld NJ. A brain region in insects that supervises walking. *Prog Brain Res.* 1999; 123:273–284. [PubMed: 10635723]
- Strausfeld, NJ. Arthropod brains: evolution, functional elegance, and historical significance. Harvard University Press; Cambridge, MA: 2012.
- Strausfeld NJ, Bassemir UK. The organization of giant horizontal-motion-sensitive neurons and their synaptic relationships in the lateral deutocerebrum of *Calliphora erythrocephala* and *Musca domestica*. *Cell Tiss Res.* 1985; 242:531–550.
- Strausfeld NJ, Lee JK. Neuronal basis for parallel visual processing in the fly. *Vis Neurosci.* 1991; 7:13–33. [PubMed: 1931797]
- Strausfeld NJ, Okamura J-Y. Visual system of calliphorid flies: organization of optic glomeruli and their lobula complex efferents. *J Comp Neurol.* 2007; 500:166–188. [PubMed: 17099891]
- Straw AD. Vision Egg: an open-source library for real-time visual stimulus generation. *Front Neuroinform.* 2008; 2:4. doi: 10.3389/neuro.11.004.2008. [PubMed: 19050754]
- Vitzhum H, Müller M, Homberg U. Neurons of the central complex of the locust *Schistocerca gregaria* are sensitive to polarized light. *J Neurosci.* 2002; 22:1114–1125. [PubMed: 11826140]
- Wada S, Kanzaki R. Neural control mechanisms of the pheromone-triggered programmed behavior in male silk-moths revealed by double-labeling of descending interneurons and a motor neuron. *J Comp Neurol.* 2005; 484:168–182. [PubMed: 15736224]
- Wehner R. “Matched filters”—neural models of the external world. *J Comp Physiol A.* 1987; 161:511–531. [PubMed: 3316619]
- Williams JLD. Anatomical studies of the insect central nervous system: a ground-plan of the midbrain and an introduction to the central complex in the locust, *Schistocerca gregaria* (Orthoptera). *J Zool Lond.* 1975; 176:67–86.
- Wu CL, Xia S, Fu TF, Wang H, Chen YH, Leong D, Chiang AS, Tully T. Specific requirement of NMDA receptors for long-term memory consolidation in *Drosophila* ellipsoid body. *Nat Neurosci.* 2007; 10:1578–1586. [PubMed: 17982450]
- Young JM, Armstrong JD. Structure of the adult central complex in *Drosophila*: organization of distinct neuronal subsets. *J Comp Neurol.* 2010; 5189:1500–1524. [PubMed: 20187142]

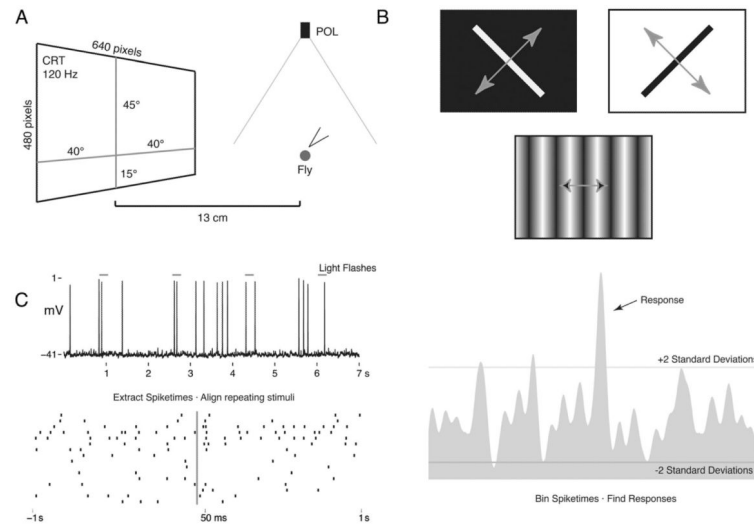


Figure 1.

Experimental setup and data analysis. **A:** Schematic showing the position of the stimulus presentation monitor (CRT) and the overhead polarized light source (POL). Flies were placed 13 cm from the CRT screen, which subtended $80^\circ \times 60^\circ$ of the frontal visual field. **B:** Examples of CRT stimuli. Gray arrows represent the direction of motion. **C:** Example analysis of light flash response. Spike times are extracted from the voltage trace and aligned according to stimulus onset (raster plot). Spike times are binned and smoothed (peristimulus time histogram; PSTH). The period prior to the stimulus is used to calculate background firing rate and variability. Two standard deviations above or below the mean unstimulated firing rate was used as the threshold for changes in activity to be judged a response.

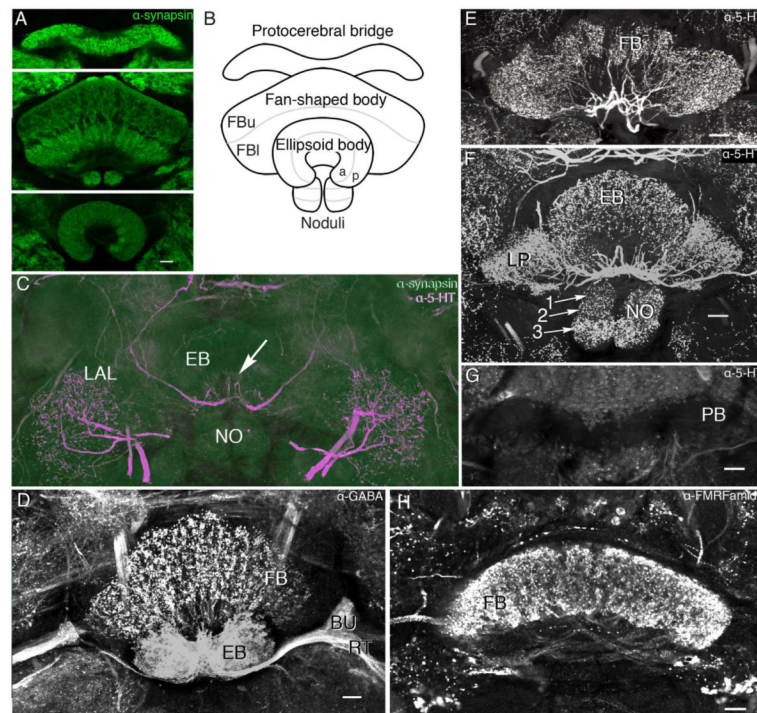


Figure 2.

Organization of the central complex of *Neobellieria bullata*. **A:** Antisynapsin staining of the protocerebral bridge, fan-shaped body (FB), noduli (NO), and ellipsoid body (EB). **B:** Schematic of central complex structures viewed frontally (ventral according to the neuraxis) showing the division of the fan-shaped body into upper (FBu) and lower (FBI) divisions, the EB into anterior (a) and posterior (p) rings, and the NO into three layers. **C:** Antisynapsin (green) and antiserotonin (5-HT; magenta) staining of an oblique section through the NO, EB, and lateral accessory lobes (LAL) showing three compartments of the NO (I, II, III), and the EB divided into two rings, anterior (a) and posterior (p), based on antisynapsin staining. Labeling with antisynapsin and anti-5-HT reveals a network of serotonin-like immunoreactive arbors innervating the LAL and two axons entering the EB, where they provide radiating branches (arrow). **D:** Oblique frontal section showing dense γ -aminobutyric acid (GABA)-like immunoreactivity in the EB, bulbs (BU), and ring neuron tract (RT) as well as a layer of anti-GABA immunoreactivity in the FB. **E:** Oblique frontal section through the FB showing processes of neurons labeled with anti-5-HT arborizing within modules of the FB. **F:** Frontal section through the EB, NO, and lateral protuberances (LP) of the FB show extensive serotonin-like immunoreactivity. The noduli are shown divided into three discrete zones (arrows 1–3). **G:** Frontal section through the protocerebral bridge showing it devoid of serotonergic innervation. **H:** Horizontal section through the FB showing dense FMRamide-like immunoreactivity in all modules and the fibers that interconnect them. Scale bars = 20 μ m. [Color figure can be viewed in the online issue, which is available at wileyonlinelibrary.com.]

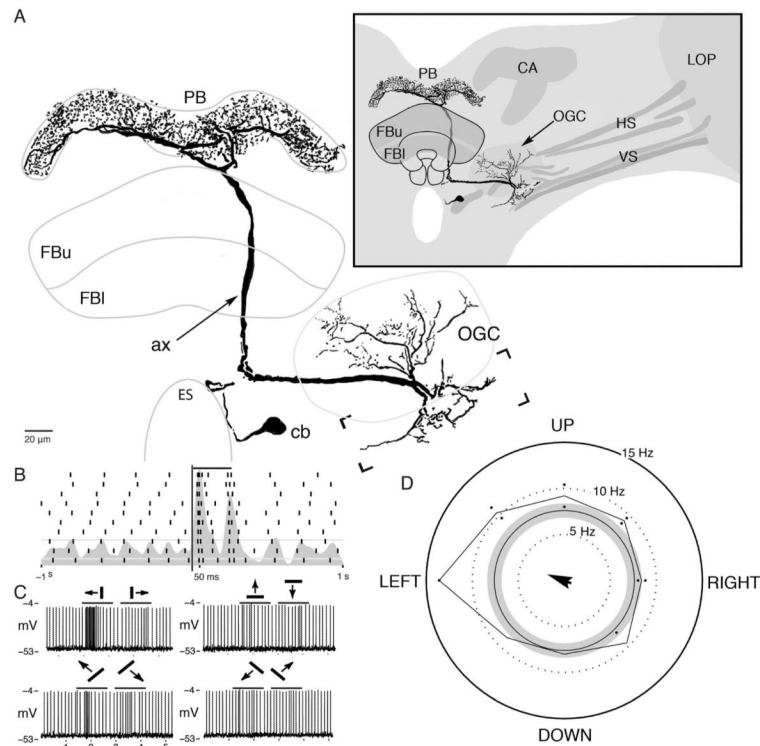


Figure 3.

Morphology and response properties of the optic glomeruli-protocerebral bridge neuron. **A:** The neuron originates from a cell body (cb) close to the esophageal foramen (ES). The neuron's dendrites within the ventrolateral protocerebrum extend within the optic glomerular complex (OGC) and to axon collaterals of lobula plate outputs (bracketed area). These elements are diagrammed as fluorescent negative profiles (**inset**). The neuron's axon (ax) extends behind the fan-shaped body (FBU, FBI) to reach the protocerebral bridge, where it provides small, beaded terminal processes across the entire neuropil (PB). **B:** Raster plot showing the spiking activity of this neuron during 10 repeats of a light flash presented from overhead. Bar indicates period of stimulus. **C:** Example voltage traces recorded during moving bar stimulus. **D:** Directional preference plot for a white bar moving across a black background. The difference in firing rate in response to a bar moving along its preferred direction is greater than 2 standard deviations above the unstimulated rate, but the shape of this distribution is not significantly different from a uniform distribution by the Rayleigh test. Arrow originating from the center indicates this neuron's preferred direction. Its length is proportional to the test statistic calculated by the Rayleigh test ($n = 193$, $r = 0.084$, $P > 0.1$).

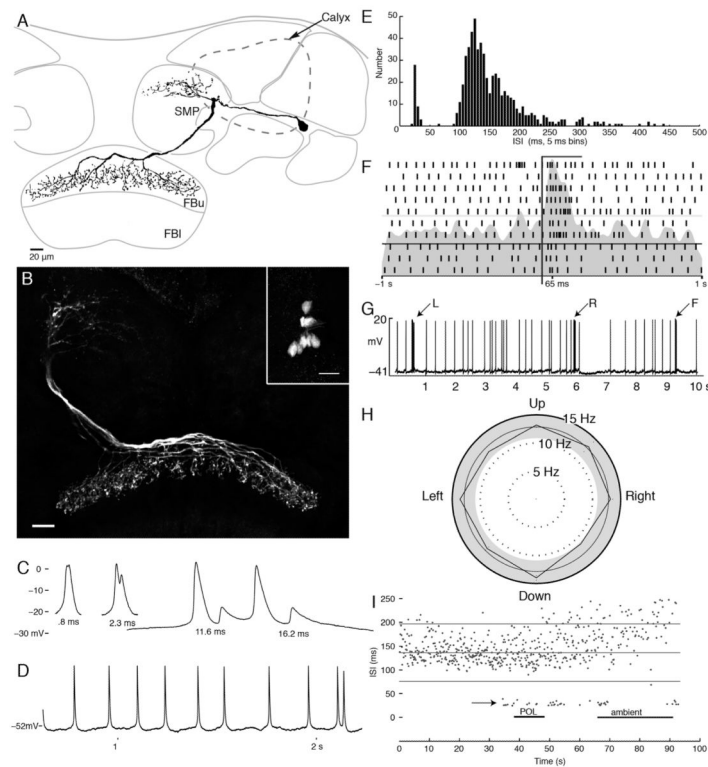


Figure 4. Tangential neurons of the fan-shaped body. **A:** Camera lucida reconstruction of a tangential neuron with arbors in the superior protocerebrum (SMP) and branches that span a stratum of the upper division of the fan-shaped body (FBU). **B:** Confocal stack showing the morphology of eight tangential neurons filled by dye injection into a single neuron. Inset shows eight cell bodies brightly labeled. **C:** Examples of the double spike waveforms of various latencies. **D:** Example voltage trace showing regular spiking activity interrupted by doublets. **E:** Histogram of observed interspike intervals (ISIs). The doublets form a separate population of spikes with ISIs < 50 msec. **F:** Raster plot showing spiking activity during 10 repeats of a light flash presented from overhead. Bar indicates period of stimulus. **G:** Example voltage trace from one tangential neuron showing the change in firing activity in response to air puffs to the left (L) and right (R) sides and from the front (F) of the head. **H:** Direction preference plot for moving bar stimulus. This stimulus has no effect on this cells firing (Rayleigh test, $n = 257$, $r = 0.006$, $P > 0.05$). **I:** ISIs (ordinate) plotted as they occurred for 100 seconds of the experiment. Doublets (short ISIs) occurred at the moment of change of the stimulus modality. Scale bars = 20 μm .

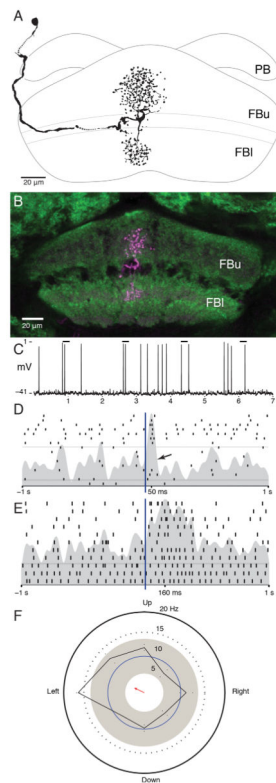


Figure 5.

Pontine neurons. **A:** Camera lucida reconstruction of a pontine neuron in the fan-shaped body that connects two layers within one module. **B:** Confocal stack showing the location of this neuron in the fan-shaped body. **C:** Example of spiking response to light flash stimuli. Bars indicate lights on. **D:** Raster plot showing an excitatory response to lights on and trials from the middle of the recording during which this stimulus failed to produce a change in firing rate (arrow). **E:** Raster plot showing a tonic response to a change in illumination. In this neuron, the increase in firing rate lasted for the duration of lights on. **F:** Direction preference plot for a white bar on a black background. Motion to the left produces an increase in firing rate greater than 2 standard deviations above the background rate, and the shape of this distribution is significantly different from random (Rayleigh test, $n = 202$, $r = 0.156$, $P < 0.05$). Scale bars = 20 μm . [Color figure can be viewed in the online issue, which is available at wileyonlinelibrary.com.]

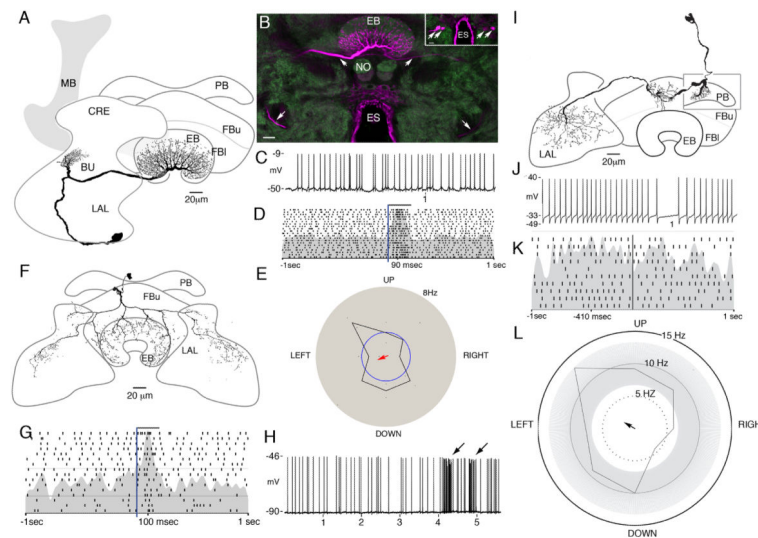


Figure 6.

Ring neurons of the ellipsoid body. **A:** Camera lucida reconstruction of a ring neuron with extensive branches in the ellipsoid body, a small tuft in the crepine neuropil (CRE) lying above the lateral accessory lobe (LAL), and a cell body at the lower margin of the LAL, posterior to the antennal lobes (not shown in this plane of section). **B:** Confocal stack showing strongly labeled arbors in the posterior ring of the ellipsoid body and a prominent neurite (arrow, middle upper left). Also visible is a faint contralateral neurite entering the ellipsoid body from the opposite side (arrow). This more weakly labeled neuron has the same morphology as the more strongly labeled nerve cell (lower arrows indicate their symmetrical paths to their cell body locations). The **inset** shows two pairs of cell bodies, one in each brain half, which have been filled with neurobiotin injected into the single neuron. **C:** Example voltage trace illustrating the variability in this neurons unstimulated activity. **D:** Raster plot showing an increase in firing rate in response to an increase in illumination (bar). **E:** Motion response of this cell for a black bar on a white background. The firing rate during the stimulus presentation is well within the variability of background firing rate (gray area), and the shape of this distribution is not significantly different from random (Rayleigh test, $n = 67$, $r = 0.105$, $P > 0.05$). **F:** Camera lucida reconstruction of an extrinsic ring neuron with extensive arbors in both LALs. The morphology of this cell corresponds to that of the ExR1 cells described by Hanesch et al. (1989). **G:** Raster plot showing response to flashed light stimuli. **H:** Voltage trace showing response to air current directed at head (arrows). **I:** Camera lucida reconstruction of a neuron connecting the protocerebral bridge, the fan-shaped body, and the contralateral LALs. **J:** Example voltage trace. **K:** Raster plot showing no response to changes in illumination. **L:** Directional tuning in response to a black bar presented on a white background. The cell is excited by movement to the upper left and inhibited by the bar moving in the opposite direction. This distribution is significantly different from random (Rayleigh test, $n = 170$, $r = 0.158$, $P < 0.05$). Scale bars 20 μm .

[Color figure can be viewed in the online issue, which is available at wileyonlinelibrary.com.]













TABLE 1

Antibodies Used in This Study

Antibody	Immunogen	Manufacturer	Concentration
FMRFamide	FMRFamide-thyroglobulin	Provided by Eve Marder Marder et al. (1987)	1:100
GABA	Y-aminobutyric acid conjugated to BSA	Sigma A2052 Rabbit polyclonal	3:1000
Serotonin	Serotonin coupled to bovine serum albumin with paraformaldehyde	Immunostar 20080 Rabbit polyclonal	3:1000
Synapsin	Drosophila SYNORF1, GSA fusion protein representing the conserved 5' end of Synapsin cDNA	Developmental Studies Hybridoma Bank 3c11 Mouse Monoclonal	1:100

TABLE 2

Morphology of Neuronal Cell Types Recorded in These Experiments¹

Cell Type	Protoocerebrum			Central Complex			References				
	Figure	Superior	Lateral	PB	FB	EB		L/AL	N	Response	
Protocerebral Bridge Input	3								2	LB	
Tangential Neurons	4							14	L _A (n = 1)	Hanesch Fig. 22g	
Ring Neurons	6a								1	L	Hanesch Fig. 21b
	6b								1	L _A	Hanesch Fig. 21a
Pontine Neurons	5							5	LB	Hanesch Fig. 9a-b	
Horizontal Fibers	6l							1	B	Hanesch Fig. 6a	

Vertical bars represent smooth terminals while filled circles represent blebbed arborizations. Responses are: L - Light Flashes, B - Moving Bar, A - Air Puffs. The references column provides the figure number from Hanesch et al., 1989 that depicts the equivalent cell type in *Drosophila*.